Proceedings of the Korean Society Autumn Meeting
Seoul, Korea, 1999

A Capacitance Tomography for Two-phase Analysis using Feedforward Neural Networks

Jae Young Lee
HanDong University
Pohang, Kyungpuk, Korea,791-940 jylee7@han.ac.kr

Abstract

This article represents an algorithm to reconstruct cross-sectional distribution the capacitance tomography sensor. The electric field in the test tube is calculated by a newly proposed PDE solver based on artificial neural network. Newton-Raphson method minimizes the square of error between the measured and calculated capacitance signals for the back projection of tomographe image.

The present PDE solver within 10^{-5} accuracy could successfully identify electric field in the test tube. Also, for the good initial guess, the back projection was made efficiently to identify well the cross sectional distribution of void for the annular flow, core flow, and stratified flow.

Key word : Capacitance Tomography, Back Projection, Partial Differential Equations, Neural Networks,

1. INTRODUCTION

The progress in the electric tomography technology expands fast in recent[1]. Among them, the capacitance tomography[2] is studied here to validate its applicability to the two-phase flow in the nuclear industry and to provide a new software for the image reconstruction for the better utilization. As far as the author's known, the heavy calculation burden to get the tomography image, normal to every inverse problem, generates a negative sight for its use in the process industry. Also, the low level capacitance signal due to its inverse relation to the distance between the electrodes needs a very sophisticate electronics of high accuracy and strong resistance against noise. In this paper, the problem related to the software, computational burden and accuracy, is investigated by preparing a new PDE solver for the electric field calculation.

The direct inversion tried at the beginning stage of this technique is now improved by adopting the finite difference[3] or element method[4] with a optimization technique. The progress head on development of more accurate and fast PDE solver and optimization technique. Also, Mayngger[5] proposed a table lookup method for real time application with remarkable accuracy. Artificial neural network[6] has been tried by using its learning capability to reproduce image.

As one of trial in this progress, the present study is designed to develop a system with new PDE solver and to study its performance for the capacitance tomography. The workability in the parallel processor and mesh independency are considering factor in choosing the PDE solver. Since the computational load for solving the difference equations increases very fast as the number of discrete points becomes large. Before implementing to the parallel computer, the present paper want to report the feasible performance of the present PDE system based on the artificial neural network for the capacitance tomography.

2. Electric Field Computer Tomography system

Recent progress in the electric tomography give a promise of possible application to the process industry for the control purpose. After inventing the capacitance tomography with 8 rectangular electrodes, its basic structure is not too much evolved yet. In the present study, the 8 electrodes are adopted to the 5.08 cm in inner diameter tube with standard coupling assembly is developed. their excitement and data acquisition are driven by the electric circuit developed for this purpose. Figures 1 and 2 show the capacitance tomography and driving electronics[3]

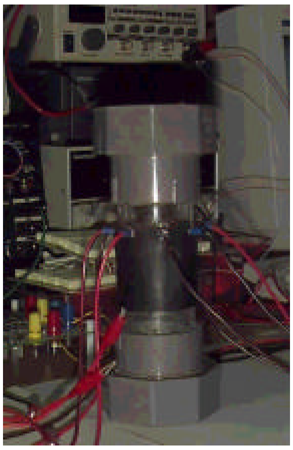

Fig.1. The capacitance tomography sensor developed

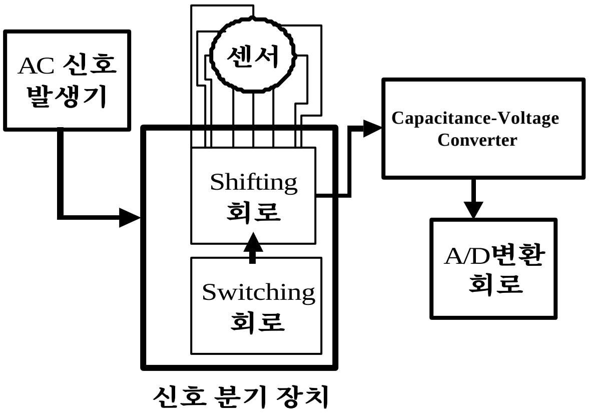

Fig.2 The conceptual drawing of electronics for the capacitance tomography sensor

3. Development of the analysis tool

3.1 The governing Equation for the electric tomography

The electric field in the test space is determined by the well known Poisson's equation as

$$\nabla \cdot \varepsilon(\boldsymbol{x}) \nabla \phi = - \rho(\boldsymbol{x}) \qquad (1)$$

where ε is the dielectric constant, ϕ is the electric potential, and ρ is the charge density. Due to Gauss law, the inner space, the electric charge is not accumulated except boundary, i.e. the surface of the electrode. The charge accumulated at the surface of the electrodes I and j could be measured by the capacitance:

$$C_{i,j} = \frac{\int\int \varepsilon \boldsymbol{E} \cdot d\boldsymbol{S}}{\phi_i - \phi_j} \tag{2}$$

The problem is simply stated as determination of the dielectric constant profile in the test space using the measured capacitance using the above governing equation for electric field.

3.2 PDE Solver by neural Networks

Most of the previous work in solving differential equations using neural networks is restricted to the case of solving the linear systems of algebraic equations which result from the discretization of the domain. The solution of a linear system of equations is mapped onto the architecture of a Hopfield neural network. The minimization of the network's energy function provides the solution to the system of equations[1, 2]. However, in this study, a new PDE based on a feedforward neural network is introduced.

Considering the following general differential equation:

$$G(\vec{x}, \Psi(\vec{x}), \nabla\Psi(\vec{x}), \nabla^2\Psi(\vec{x})) = 0, \quad \vec{x} \in D \tag{3}$$

subject to certain boundary conditions (for instance Dirichlet and/or Neumann), where $\vec{x} = (x_1, \ldots, x_n) \in R^n$, $D \subset R^n$ denotes the definition domain and $\Psi(\vec{x})$ is the solution to be computed. To obtain a solution to the above differential equation the collocation method is adopted which assumes a discretization of the domain D and its boundary S into a set points $\hat{D}$ and $\hat{S}$ respectively. The problem is then transformed into the following system of equations:

$$G(\vec{x_i}, \Psi(\vec{x_i}), \nabla\Psi(\vec{x_i}), \nabla^2\Psi(\vec{x_i})) = 0, \quad \forall \vec{x_i} \in \hat{D} \tag{4}$$

subject to the constraints imposed by the B.Cs.

If $\Psi_t(\vec{x}, \vec{p})$ denotes a trial solution with adjustable parameters $\vec{p}$, the problem is transformed to:

$$\min_{\vec{p}} \sum_{x_i \in D} G(\vec{x_i}, \Psi(\vec{x_i}, \vec{p}), \nabla\Psi(\vec{x_i}, \vec{p}), \nabla^2\Psi(\vec{x_i}, \vec{p}))^2 \tag{5}$$

subject to the constraints imposed by the B.Cs.

In the proposed approach the trial solution Ψ_t employs a feedforward neural network and the parameters $\vec{p}$ correspond to the weights and biases of the neural architecture. We choose a form for the trial function $\Psi_t(\vec{x})$ such that by construction satisfies the BCs. This achieved by writing it as a sum of two terms:

$$\Psi_t(\vec{x}) = A(\vec{x}) + F(\vec{x}, N(\vec{x}, \vec{p})) \tag{6}$$

where $N(\vec{x}, \vec{p})$ is a single-output feedforward neural network with parameters $\vec{p}$ and n input units fed with the input vector $\vec{x}$.

The term $A(\vec{x})$ contains no adjustable parameters and satisfies the boundary conditions. The second term F is constructed so as not to contribute to the BCs, since $\Psi_t(\vec{x})$ must also satisfy them. This term employs a neural network whose weights and biases are to be adjusted in order to deal with the minimization problem. The efficient minimization of Eq.3 can be considered as a procedure of training the neural network where the error corresponding to each input vector $\vec{x}_i$ is the value $G(\vec{x}_i)$ which has to become zero. Computation of this error value involves not only the network output (as is the case in conventional training) but also the derivatives of the output with respect to any of its inputs. Therefore, in computing the gradient of this error with respect to the network weights, we need to compute not only the gradient of the network but also the gradient of the network derivatives with respect to its inputs.

Consider a multilayer perceptron with n input units, one hidden layer with H sigmoid units and a linear output unit.

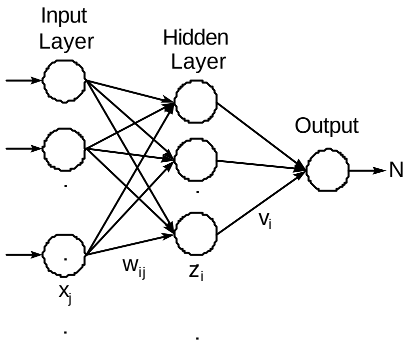

Fig.3 Multilayer Perceptron with H hidden units and a output unit.

For a given input vector $\vec{x} = (x_1, \ldots, x_n)$ the output of the network is

$$N = \sum_{i=1}^{H} v_i \sigma(z_i) \tag{7}$$

where $z_i = \sum_{j=1}^{n} w_{ij} x_j + u_i$ w_{ij} denotes the weight from the input unit j to the hidden unit i, v_i denotes the weight from the hidden unit i to the output, u_i denotes the bias of hidden unit i and $\sigma(z)$ is the sigmoid transfer function. The gradient of the network derivatives with respect to its input, x_j is

$$\frac{\partial N}{\partial x_j} = \sum_{i=1}^{H} v_i w_{ij} \sigma'(z_i) \tag{8}$$

Therefore we have

$$\frac{\partial^k N}{\partial x_j^k} = \sum_{i=1}^{H} v_i w_{ij}^k \sigma_i^{(k)} \tag{9}$$

where $\sigma_i = \sigma(z_i)$and $\sigma^{(k)}$ is the k-th order derivative of the sigmoid.

This leads to

$$\frac{\partial^{\lambda_1} N}{\partial x_1^{\lambda_1}}\frac{\partial^{\lambda_2} N}{\partial x_2^{\lambda_2}}\cdots\frac{\partial^{\lambda_n} N}{\partial x_n^{\lambda_n}} = \sum_{i=1}^{H} v_i (w_{i1}^{\lambda_1} w_{i2}^{\lambda_2}\cdots w_{in}^{\lambda_n})\sigma_i^{(\lambda_1)}\sigma_i^{(\lambda_2)}\cdots\sigma_i^{(\lambda_n)} = \sum_{i=1}^{H} v_i P_i \sigma_i^{(\Lambda)} \tag{10}$$

where $P_i = \prod_{k=1}^{n} w_{ik}^{\lambda_k}$ and $\Lambda = \sum_{i=1}^{n}\lambda_i$

Equation (6) denotes that the derivative of the original network with respect to any of its outputs is equivalent to a feedforward neural network $N_g(\vec{x})$ with one hidden layer.

Table 1. Comparison the network parameters between original and equivalent network.

	Original Network	Equivalent Network
Output of the network	N	N_g
The weight from the input unit j to the hidden unit i	w_{ij}	w_{ij}
The bias of hidden unit i	u_i	u_i
The weight from the hidden unit i to the output	v_i	v_iP_i
Transfer function	σ_i	$\sigma_i^{(\Lambda)}$

Therefore the gradient of N_g with respect to the parameters of the original network can be easily obtained as:

$$\frac{\partial N_g}{\partial v_i} = P_i \sigma_i^{(\Lambda)} \tag{11}$$

$$\frac{\partial N_g}{\partial u_i} = \frac{\partial}{\partial u_i}\left(\sum_{i=1}^{H} v_i P_i \sigma_i^{(\Lambda)}\right) = v_i P_i \sigma_i^{(\Lambda+1)} \tag{12}$$

$$\begin{aligned}\frac{\partial N_g}{\partial w_{ij}} &= \sum_{f=1}^{H} v_f\Big[P_f \sum_{m=1}^{n} x_m \delta_{jm}\sigma_f^{(\Lambda+1)} + \sum_{m=1}^{n}\lambda_m w_{fm}^{\lambda_m-1}\delta_{jm}\Big(\prod_{k=1,\,k\neq j}^{n} w_{fk}^{\lambda_k}\Big)\sigma_f^{(\Lambda)}\Big]\delta_{if} \\ &= \sum_{f=1}^{H} v_f P_f x_j \sigma_f^{(\Lambda+1)} + \sum_{f=1}^{H} v_f \lambda_j w_{fj}^{\lambda_j-1}\Big(\prod_{k=1,\,k\neq j}^{n} w_{fk}^{\lambda_k}\Big)\sigma_f^{(\Lambda)}\delta_{if} \\ &= x_j v_i P_i \sigma_i^{(\Lambda+1)} + v_i \lambda_j w_{ij}^{\lambda_j-1}\Big(\prod_{k=1,\,k\neq j}^{n} w_{ik}^{\lambda_k}\Big)\sigma_i^{(\Lambda)}\end{aligned} \tag{13}$$

Let us apply the above algorithm to the Poisson's equation:

$$\frac{\partial^2}{\partial x^2}\Psi(x,y) + \frac{\partial^2}{\partial y^2}\Psi(x,y) = f(x,y) \tag{14}$$

$x \in [0,1]$, $y \in [0,1]$ with Dirichlet BC:

$$\Psi(0,y) = f_0(y)\ ,\ \Psi(1,y) = f_1(y)\ ,\ \Psi(x,0) = g_0(x)\ ,\ \Psi(x,1) = g_1(x). \tag{15}$$

The trial solution is written as:

$$\Psi_t(x,y) = A(x,y) + x(1-x)y(1-y)N(x,y,\vec{p}) \tag{16}$$

where A(x,y) is chosen so as to satisfy the BC, namely:

$$\begin{aligned}A(x,y)= &\ (1-x)f_0(y)+xf_1(y)\\ &+(1-y)\{g_0(x)-[(1-x)g_0(0)+xg_0(1)]\}+y\{g_1(x)-[(1-x)g_1(0)+xg_1(1)]\}\end{aligned} \tag{17}$$

In PDE problems the error to be minimized is given by:

$$E[\vec{p}]=\sum_i\left\{\frac{\partial^2}{\partial x^2}\Psi(x_i,y_i)+\frac{\partial^2}{\partial y^2}\Psi(x_i,y_i)-f(x_i,y_i)\right\}^2 \tag{18}$$

where (x_i, y_i) are points in $[0,1]\times[0,1]$

We consider boundary value problem with Dirichlet BCs, Following problem was defined on the domain $[0,1]\times[0,1]$ and in order to perform training we consider a mesh of 100 points obtained by considering 10 equidistant points of the domain [0,1] of each variable.

In analogy the neural architecture was considered to be a multilayer perceptron with two inputs (accepting the coordinates x and y of each point), 10 sigmoid hidden units and one linear output unit. The sigmoid activation of each hidden unit is $\sigma(x)=\frac{1}{1+e^{-x}}$ The exact analytic solution $\Phi_a(\vec{x})$ was known in advance. Therefore we test the accuracy of the obtained solutions by computing the deviation $\Delta\Phi(\vec{x})=\Phi_t(\vec{x})-\Phi_a(\vec{x})$ To perform the error minimization we employed the steepest descent method.

3.3 The Back Projection Method

The back projection to determine the tomographe image using the capacitances measured form the electrodes is follows the well known optimization technique of Newton-Raphson.

The procedures are made to minimize the error between the measured one and calculated one by adjusting the dielectric constants in the mesh.

Discretization of Eq.(2) results in the following algebraic relation for calculated capacitance of n th sequential pairs between electrodes as:

$$C_{n,C}=C_{I,J}=\sum_{i=1}^{n}\sum_{j=1}^{m}a_{i,j}\varepsilon_{i,j}\phi_{i,j} \tag{19}$$

where n is the sequential number of electrode pairs up to 28 for 8 electrodes, the subscripts I,J are the sequential number of electrode and i,j is the indicating number of mesh.

The objective function to be minimized is the total summation of the all errors between the measured capacitance and the calculated one:

$$O=\sum_1^{28}E_n^2=\sum_1^{28}(C_{n,M}-C_{n,C})^2 \tag{20}$$

$$O=\sum_{i=1}^{n}\sum_{i=1}^{n}A_{i,j}\varepsilon_{i,j}^2\phi_{i,j}^2+B_{i,j}\varepsilon_{i,j}\phi_{i,j}+C_{i,j} \tag{21}$$

The minimization of the objective function is made as :

$$O^{k+1}-O^k=\left[\frac{\partial O}{\partial\varepsilon_{i,j}}\right]^k(\varepsilon_{i,j}^{k+1}-\varepsilon_{i,j}^k) \tag{22}$$

Since the k+1 th stage objective function should be 0, the changed dielectric constant is determined as

$$\varepsilon_{i,j}^{k+1}=\varepsilon_{i,j}^{k}-\frac{O^{k}}{\left[\dfrac{\partial O}{\partial \varepsilon_{i,j}}\right]^{k}} \tag{23}$$

4. Results and Discussions

4.1 Accuracy of the PDE solver

To evaluate the present PDE solver, the following two coupled PDEs having analytic solutions are used::

$$\begin{cases} \dfrac{\partial^2 \Phi_1}{\partial x^2}+\dfrac{\partial^2 \Phi_1}{\partial y^2}-2\Phi_2=e^{-x}(x+y^3+12y-2)-2(2-\pi^2y^2)x^3 \\ \\ \dfrac{\partial^2 \Phi_2}{\partial x^2}+\dfrac{\partial^2 \Phi_2}{\partial y^2}+\Phi_1\Phi_2+x^3\Phi_1=2x(6-3\pi^2y^2-\pi^2x^2)+x^3e^{-x}(3-\pi^2y^2)(x+y^3+6y) \end{cases} \tag{24}$$

with $x,y\in[0,1]$ and Dirichlet Boundary conditions:

$$\begin{cases} \Phi_1(0,y)=y^3+6y & , \quad \Phi_1(1,y)=e^{-1}(1+y^3+6y) \\ \Phi_1(x,0)=xe^{-x} & , \quad \Phi_1(x,1)=(x+7)e^{-x} \\ \Phi_2(0,y)=0 & , \quad \Phi_2(1,y)=(2-\pi^2y^2) \\ \Phi_2(x,0)=2x^3 & , \quad \Phi_2(x,1)=x^3(2-\pi^2) \end{cases} \tag{25}$$

Its analytic solutions are as follows:

$$\begin{cases} \Phi_1=e^{-x}(x+y^3+6y) \\ \\ \Phi_2=(2-\pi^2y^2)x^3 \end{cases} \tag{26}$$

Accuracy results are presented in Figures 4, 5 for the training points with a reasonable range..

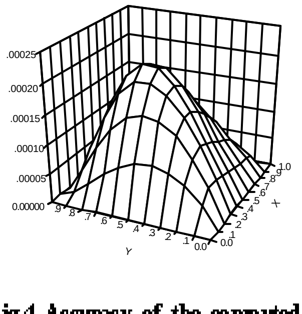

Fig.4 Accuracy of the computed solutionat the training points, $|\Delta\Phi_1|$

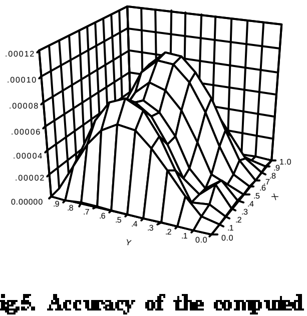

Fig.5. Accuracy of the computed solution at the training points, $|\Delta\Phi_2|$

4.2 Electiric field in the capacitance tomography

The PDE solver is applied to Poison equation of the cylindrical geometry and successfully calculate electric field as shown in the Figs. 10 and 11. where the filed spikes generated from the electrode of applying voltages and that attaching to the ground. Figure 6 shows the electric field when the tube is filled with water fully where the order of electrodes paring are 1-2, 1-3, 1-4, 1-5, 1-6, 1-7, 1-8, respectively. Also, the electric field for the tube filled in half with water in an stratified flow way are presented in the Fig7 Since the low capacitance in the PF level prevent us from recognize its difference in a sight.

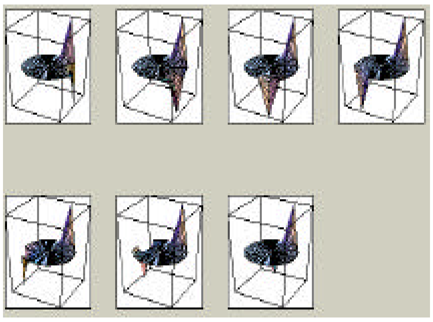

Fig.6 the electric field calculated for the fully filled cylinder with water

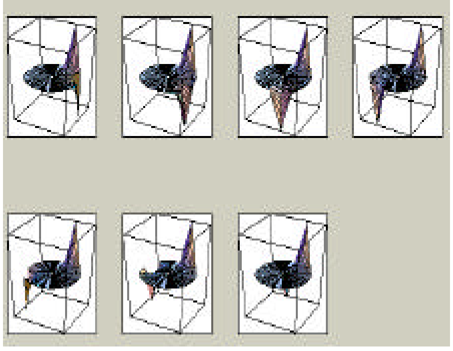

Fig.7 The electric field calculated for for the half-filled cylinder with water

4.3 Back Projection Results of the Two-phase tomography

Using the developed electric field calculator, the back projection is made by changing the dielectric constant in the each cell. To achieve fast convergence, The pattern correspondent to the flow pattern in specific is identified before operation. In order to see the error propagation to the back projection, 28th random noises are generated for each electrode parings and added to the capacitance calculated to impose the observation error.

As shown in Fig. 8, the stratified flow is well reconstructed by the present algorithm. The noise affect the result by removing two nodes of water in the mesh which is less than 5% of error in terms of void fraction. Figure 9 shows the results of slug flow where the error is widely spread around the circular mesh. But is hardly to set the epsilon value using the water and air only. Figure 10 shows that the core flow resulting in the very low capacitance signals, but its image could be successfully projected in the backward direction. The present algorithm successfully projects the patterns showing in Fig.11. However, it is still difficult to identify tiny bubbles. For the practical usage, algorithm should be improved in both speed and accuracy.

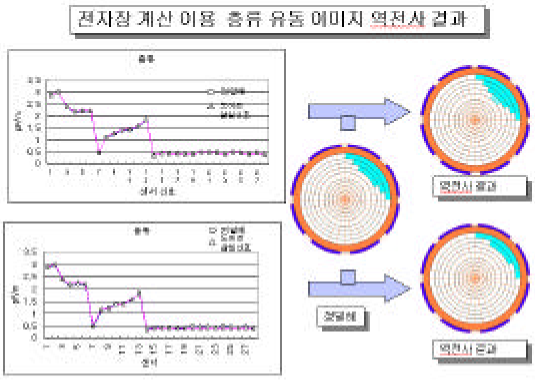

Fig 8 The tomography image for the stratified flow

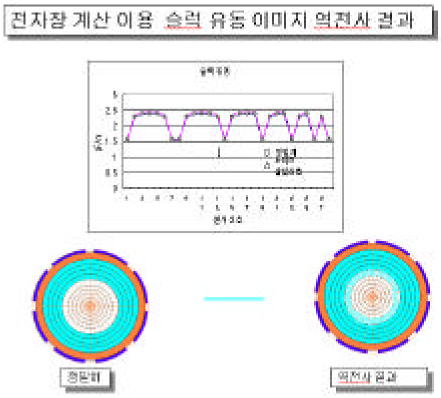

Fig.9 The tomogrpahy image for the slug flow

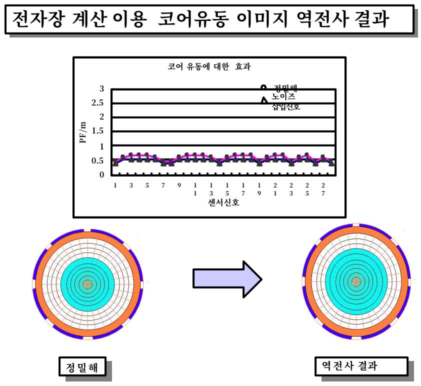

Fig 10 The tomography image for the core flow

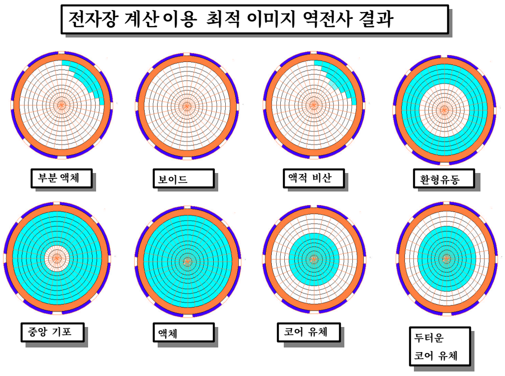

Fig.11 The tomogrpahy image for various flow patterns

5. Conclusions

In the present study, a software for capacitance tomography having a new PDE solver based on the artificial neural network of parallel processing capability and independency from mesh.

The cross sectional distributions of gas in the test tube for various flow regimes such as the stratified flow, annular flow, core flow are identified well with the Newton-Raphson optimization by mimimize the capacitance error between measured and the calculated.

Through the present study, it could be concluded that the capacitance tomography could be implemented by the present algorithm. However, for the tiny bubbles, study should be extended.

Acknowledgement

The financial support form the Ministry of Science and Technology in the program of the fundamental nuclear studies are greatly acknowledged.

REFERENCES

[1] M.D. Baek and P.A. William, " Process Tomography: a European Innovation and its applications, " Measurement and Science and Technology vol 7 pp 215-224(1996)

[2] Oyyind Issaksen, " A review of reconstruction technique for capacitance tomography," Measurement Science Technology, vol. 7, pp 325-337 (1996)

[3] T.J.Yorkey, J.C. Webster, W.J. Tompkins, " An Improved perturbation technique for electrical impedence imaging with some criticisms. IEEE trans. on Biomedical Eng. Vol.BME-34, No.11, (1987)

[4] O.C. Jones, J.T. Lin, L.Ovacik, H.J.Shu, " Impedence imaging relative to gas-liquid systems," Nuclear Eng.& Design vol. 141 pp159-176 (1996)

[5] Klug and Maynger F, " Impedence based flow reconstruction- a novel flow component measuring technique for multi-phase flow," Nuclear Engineering and Design, vol 146 pp35-42 (1997)

[6] Wang, L. and Mendel J.M., Structured trainable networks for matrix algebra, IEEE Int. Joint Conference on Neural Networks, vol. 2, pp. 125-128, 1990.

[7] Yentis, R. and Zaghoul, M.E., VLSII Implementation of Locally Connected Neural Network for Solving Partial Differential Equations, IEEE Trans on Circuits and Systems-I, vol. 43, no. 8, pp. 687-690, 1996.

[8] Jae Young Lee, Development of computer tomography for two-phase flow, Final Report for the fundamental study on nuclear engineering, MOST (1999)